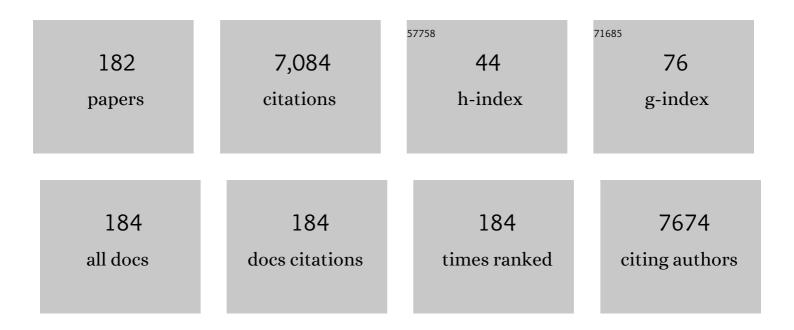


List of Publications by Year in descending order

Source: https://exaly.com/author-pdf/610773/publications.pdf Version: 2024-02-01



#	Article	IF	CITATIONS
1	CO2 hydrogenation to high-value products via heterogeneous catalysis. Nature Communications, 2019, 10, 5698.	12.8	571
2	Aminoâ€Assisted Anchoring of CsPbBr <sub>3</sub> Perovskite Quantum Dots on Porous g <sub>3</sub> N <sub>4</sub> for Enhanced Photocatalytic CO <sub>2</sub> Reduction. Angewandte Chemie - International Edition, 2018, 57, 13570-13574.	13.8	432
3	A Perovskite Nanorod as Bifunctional Electrocatalyst for Overall Water Splitting. Advanced Energy Materials, 2017, 7, 1602122.	19.5	369
4	Perovskite-type CsPbBr3 quantum dots/UiO-66(NH2) nanojunction as efficient visible-light-driven photocatalyst for CO2 reduction. Chemical Engineering Journal, 2019, 358, 1287-1295.	12.7	280
5	A Highly Efficient and Robust Cation Ordered Perovskite Oxide as a Bifunctional Catalyst for Rechargeable Zinc-Air Batteries. ACS Nano, 2017, 11, 11594-11601.	14.6	219
6	Aminoâ€Assisted Anchoring of CsPbBr <sub>3</sub> Perovskite Quantum Dots on Porous g <sub>3</sub> N <sub>4</sub> for Enhanced Photocatalytic CO <sub>2</sub> Reduction. Angewandte Chemie, 2018, 130, 13758-13762.	2.0	172
7	Fabrication of 3D Co-doped Ni-based MOF hierarchical micro-flowers as a high-performance electrode material for supercapacitors. Applied Surface Science, 2019, 483, 1158-1165.	6.1	156
8	Rational construction of triangle-like nickel-cobalt bimetallic metal-organic framework nanosheets arrays as battery-type electrodes for hybrid supercapacitors. Journal of Colloid and Interface Science, 2019, 555, 42-52.	9.4	131
9	Amino-Assisted NH <sub>2</sub> -UiO-66 Anchored on Porous g-C <sub>3</sub> N <sub>4</sub> for Enhanced Visible-Light-Driven CO <sub>2</sub> Reduction. ACS Applied Materials & Interfaces, 2019, 11, 30673-30681.	8.0	116
10	Highly-efficient visible-light-driven photocatalytic H2 evolution integrated with microplastic degradation over MXene/ZnxCd1-xS photocatalyst. Journal of Colloid and Interface Science, 2022, 605, 311-319.	9.4	112
11	Ultrathin 2D Ti3C2 MXene Co-catalyst anchored on porous g-C3N4 for enhanced photocatalytic CO2 reduction under visible-light irradiation. Journal of Colloid and Interface Science, 2021, 582, 647-657.	9.4	111
12	Ultrasound assisted synthesis of heterogeneous g-C3N4/BiVO4 composites and their visible-light-induced photocatalytic oxidation of NO in gas phase. Journal of Alloys and Compounds, 2015, 626, 401-409.	5.5	106
13	Enhanced performance and selectivity of CO2 methanation over g-C3N4 assisted synthesis of Ni CeO2 catalyst: Kinetics and DRIFTS studies. International Journal of Hydrogen Energy, 2018, 43, 15191-15204.	7.1	104
14	Synergistic interaction of perovskite oxides and N-doped graphene in versatile electrocatalyst. Journal of Materials Chemistry A, 2019, 7, 2048-2054.	10.3	104
15	Carbonâ€Based Electrocatalysts for Efficient Hydrogen Peroxide Production. Advanced Materials, 2021, 33, e2103266.	21.0	104
16	Construction of Z-scheme photocatalytic systems using ZnIn 2 S 4 , CoO x -loaded Bi 2 MoO 6 and reduced graphene oxide electron mediator and its efficient nonsacrificial water splitting under visible light. Chemical Engineering Journal, 2017, 325, 690-699.	12.7	94
17	Double redox process to synthesize CuO–CeO2 catalysts with strong Cu–Ce interaction for efficient toluene oxidation. Journal of Hazardous Materials, 2021, 404, 124088.	12.4	91
18	A Tailored Bifunctional Electrocatalyst: Boosting Oxygen Reduction/Evolution Catalysis via Electron Transfer Between Nâ€Doned Graphene and Perovskite Oxides, Small, 2018, 14, e1802767	10.0	85

#	Article	IF	CITATIONS
19	Obtaining well-dispersed Ni/Al2O3 catalyst for CO2 methanation with a microwave-assisted method. International Journal of Hydrogen Energy, 2017, 42, 4174-4183.	7.1	83
20	Porous Cobalt Phosphide Polyhedrons with Iron Doping as an Efficient Bifunctional Electrocatalyst. Small, 2017, 13, 1701167.	10.0	82
21	Identifying the structure of Zn-N2 active sites and structural activation. Nature Communications, 2019, 10, 2623.	12.8	79
22	Efficient visible-light photocatalytic oxidation of gaseous NO with graphitic carbon nitride (g–C3N4) activated by the alkaline hydrothermal treatment and mechanism analysis. Journal of Hazardous Materials, 2015, 300, 598-606.	12.4	76
23	A New Insight into Catalytic Ozonation with Nanosized Ce–Ti Oxides for NO <sub><i>x</i></sub> Removal: Confirmation of Ce–O–Ti for Active Sites. Industrial & Engineering Chemistry Research, 2015, 54, 2012-2022.	3.7	74
24	CeO2 supported on reduced TiO2 for selective catalytic reduction of NO by NH3. Journal of Colloid and Interface Science, 2017, 496, 487-495.	9.4	69
25	A Minireview on Nickelâ€Based Heterogeneous Electrocatalysts for Water Splitting. ChemCatChem, 2019, 11, 5913-5928.	3.7	68
26	Graphene-decorated 3D BiVO4 superstructure: Highly reactive (040) facets formation and enhanced visible-light-induced photocatalytic oxidation of NO in gas phase. Applied Catalysis B: Environmental, 2016, 193, 160-169.	20.2	64
27	Enhanced catalytic ozonation for NOx removal with CuFe 2 O 4 nanoparticles and mechanism analysis. Journal of Molecular Catalysis A, 2016, 424, 153-161.	4.8	63
28	Capture of carbon dioxide from flue gas on TEPA-grafted metal-organic framework Mg2(dobdc). Journal of Environmental Sciences, 2013, 25, 2081-2087.	6.1	61
29	Elemental mercury oxidation and adsorption on magnesite powder modified by Mn at low temperature. Journal of Hazardous Materials, 2015, 283, 252-259.	12.4	60
30	Aminated graphite oxides and their composites with copper-based metal–organic framework: in search for efficient media for CO2 sequestration. RSC Advances, 2013, 3, 9932.	3.6	59
31	In Site Growth of Crosslinked Nickel–Cobalt Hydroxides@Carbon Nanotubes Composite for a Highâ€Performance Hybrid Supercapacitor. Advanced Materials Interfaces, 2018, 5, 1800438.	3.7	56
32	Foaming behavior of microcellular foam polypropylene/modified nano calcium carbonate composites. Journal of Applied Polymer Science, 2013, 128, 3639-3651.	2.6	55
33	Simultaneous removal of NOX and SO2 with H2O2 over Fe based catalysts at low temperature. RSC Advances, 2014, 4, 5394.	3.6	53
34	In situ fabrication of amorphous TiO2/NH2-MIL-125(Ti) for enhanced photocatalytic CO2 into CH4 with H2O under visible-light irradiation. Journal of Colloid and Interface Science, 2020, 560, 857-865.	9.4	53
35	The effect of CuO loading on different method prepared CeO2 catalyst for toluene oxidation. Science of the Total Environment, 2020, 712, 135635.	8.0	52
36	One-step hydrothermal synthesis of a novel 3D BiFeWO <sub>x</sub> /Bi <sub>2</sub> WO <sub>6</sub> composite with superior visible-light photocatalytic activity. Green Chemistry, 2018, 20, 3014-3023.	9.0	51

#	Article	IF	CITATIONS
37	Ti3+ doped V2O5/TiO2 catalyst for efficient selective catalytic reduction of NOx with NH3. Journal of Colloid and Interface Science, 2021, 581, 76-83.	9.4	51
38	Effects of synthesis methods on catalytic activities of CoO x –TiO 2 for low-temperature NH 3 -SCR of NO. Journal of Environmental Sciences, 2017, 54, 277-287.	6.1	50
39	Novel Fe-doped CePO4 catalyst for selective catalytic reduction of NO with NH3: The role of Fe3+ ions. Journal of Hazardous Materials, 2020, 383, 121212.	12.4	50
40	Supramolecular Synthesis of Multifunctional Holey Carbon Nitride Nanosheet with High‣fficiency Photocatalytic Performance. Advanced Optical Materials, 2017, 5, 1700536.	7.3	49
41	Synthesis and characterization of g-C3N4/BiVO4 composite photocatalysts with improved visible-light-driven photocatalytic performance. Journal of Sol-Gel Science and Technology, 2014, 72, 443-454.	2.4	48
42	In Situ Fabrication of 3D Octahedral g <sub>3</sub> N <sub>4</sub> /BiFeWO <sub><i>x</i></sub> Doubleâ€Heterojunction for Highly Selective CO <sub>2</sub> Photoreduction to CO Under Visible Light. ChemCatChem, 2018, 10, 4578-4585.	3.7	48
43	Novel Bi <sub>2</sub> O <sub>2</sub> CO <sub>3</sub> /polypyrrole/g-C <sub>3</sub> N <sub>4</sub> nanocomposites with efficient photocatalytic and nonlinear optical properties. RSC Advances, 2017, 7, 7658-7670.	3.6	47
44	One-pot synthesis of ceria and cerium phosphate (CeO2-CePO4) nanorod composites for selective catalytic reduction of NO with NH3: Active sites and reaction mechanism. Journal of Colloid and Interface Science, 2018, 524, 8-15.	9.4	45
45	Influence of Calcination Temperature on Activity and Selectivity of Ni–CeO2 and Ni–Ce0.8Zr0.2O2 Catalysts for CO2 Methanation. Topics in Catalysis, 2018, 61, 1514-1527.	2.8	45
46	<i>In situ</i> self-assembly of zirconium metal–organic frameworks onto ultrathin carbon nitride for enhanced visible light-driven conversion of CO <sub>2</sub> to CO. Journal of Materials Chemistry A, 2020, 8, 6034-6040.	10.3	45
47	Effect of nano-Calcium Carbonate on microcellular foaming of polypropylene. Journal of Materials Science, 2013, 48, 2504-2511.	3.7	44
48	Promotion of surface oxygen vacancies on the light olefins synthesis from catalytic CO2 hydrogenation over Fe K/ZrO2 catalysts. International Journal of Hydrogen Energy, 2019, 44, 11808-11816.	7.1	44
49	Effects of Cr on the NO oxidation over the ceria–zirconia solid solution. RSC Advances, 2013, 3, 7009.	3.6	43
50	Promotional effect of Si-doped V2O5/TiO2 for selective catalytic reduction of NO x by NH3. Journal of Environmental Sciences, 2013, 25, 1703-1711.	6.1	42
51	Size- and shape-controlled synthesis and catalytic performance of iron–aluminum mixed oxide nanoparticles for NOX and SO2 removal with hydrogen peroxide. Journal of Hazardous Materials, 2015, 283, 633-642.	12.4	42
52	A Composite Catalyst Based on Perovskites for Overall Water Splitting in Alkaline Conditions. ChemElectroChem, 2019, 6, 1520-1524.	3.4	42
53	Haloid acid induced carbon nitride semiconductors for enhanced photocatalytic H2 evolution and reduction of CO2 under visible light. Carbon, 2018, 138, 465-474.	10.3	41
54	Characterization study on the promoting effect of F-doping V2O5/TiO2 SCR catalysts. RSC Advances, 2012, 2, 7906.	3.6	40

#	Article	IF	CITATIONS
55	New insight into the promoting role of process on the CeO2–WO3/TiO2 catalyst for NO reduction with NH3 at low-temperature. Journal of Colloid and Interface Science, 2015, 448, 417-426.	9.4	40
56	Recent Progress of CeO <sub>2</sub> â^'TiO <sub>2</sub> Based Catalysts for Selective Catalytic Reduction of NO <sub>x</sub> by NH <sub>3</sub> . ChemCatChem, 2021, 13, 491-505.	3.7	38
57	Treatment of carbon cloth anodes for improving power generation in a dualâ€chamber microbial fuel cell. Journal of Chemical Technology and Biotechnology, 2013, 88, 623-628.	3.2	37
58	CO2 hydrogenation to light olefins with high-performance Fe0.30Co0.15Zr0.45K0.10O1.63. Journal of Catalysis, 2019, 377, 224-232.	6.2	37
59	Construction of Nano-Fe <sub>2</sub> O <sub>3</sub> -Decorated Flower-Like MoS <sub>2</sub> with Fe–S Bonds for Efficient Photoreduction of CO <sub>2</sub> under Visible-Light Irradiation. ACS Sustainable Chemistry and Engineering, 2020, 8, 12603-12611.	6.7	34
60	One-pot fabrication of mesoporous g-C3N4/NiS co-catalyst counter electrodes for quantum-dot-sensitized solar cells. Journal of Materials Science, 2020, 55, 10712-10724.	3.7	34
61	Site-exposed Ti <sub>3</sub> C <sub>2</sub> MXene anchored in N-defect g-C <sub>3</sub> N <sub>4</sub> heterostructure nanosheets for efficient photocatalytic N <sub>2</sub> fixation. Catalysis Science and Technology, 2021, 11, 1027-1038.	4.1	34
62	A Fe single atom on N,S-doped carbon catalyst for performing N-alkylation of aromatic amines under solvent-free conditions. Journal of Materials Chemistry A, 2021, 9, 25128-25135.	10.3	34
63	Synthesis and characterization of direct Z-scheme Bi2MoO6/ZnIn2S4 composite photocatalyst with enhanced photocatalytic oxidation of NO under visible light. Journal of Materials Science, 2017, 52, 11453-11466.	3.7	31
64	Recent progress in Bi <sub>2</sub> WO <sub>6</sub> â€Based photocatalysts for clean energy and environmental remediation: Competitiveness, challenges, and future perspectives. Nano Select, 2021, 2, 187-215.	3.7	31
65	Z-scheme Caln <sub>2</sub> S <sub>4</sub> /Ag <sub>3</sub> PO <sub>4</sub> nanocomposite with superior photocatalytic NO removal performance: fabrication, characterization and mechanistic study. New Journal of Chemistry, 2018, 42, 318-326.	2.8	29
66	Facile synthesis of the Z-scheme graphite-like carbon nitride/silver/silver phosphate nanocomposite for photocatalytic oxidative removal of nitric oxides under visible light. Journal of Colloid and Interface Science, 2021, 588, 110-121.	9.4	29
67	Ni and Zn co-substituted Co(CO3)0.5OH self-assembled flowers array for asymmetric supercapacitors. Journal of Colloid and Interface Science, 2020, 573, 299-306.	9.4	28
68	Catalytic Oxidation of NO to NO2 Over Co–Ce–Zr Solid Solutions: Enhanced Performance of Ce–Zr Solid Solution by Co. Catalysis Letters, 2014, 144, 538-544.	2.6	27
69	Sodium doped flaky carbon nitride with nitrogen defects for enhanced photoreduction carbon dioxide activity. Journal of Colloid and Interface Science, 2021, 603, 210-219.	9.4	26
70	Effect of synergy between oxygen vacancies and graphene oxide on performance of TiO2 for photocatalytic NO removal under visible light. Separation and Purification Technology, 2021, 276, 119362.	7.9	26
71	Advances and Perspectives for the Application of Perovskite Oxides in Supercapacitors. Energy & Fuels, 2021, 35, 17353-17371.	5.1	26
72	Ag and MOFs-derived hollow Co3O4 decorated in the 3D g-C3N4 for creating dual transferring channels of electrons and holes to boost CO2 photoreduction performance. Journal of Colloid and Interface Science, 2022, 609, 901-909.	9.4	26

#	Article	IF	CITATIONS
73	Ferrous-based electrolyte for simultaneous NO absorption and electroreduction to NH3 using Au/rGO electrode. Journal of Hazardous Materials, 2022, 430, 128451.	12.4	26
74	Recent advance of cyclodextrins as nanoreactors in various organic reactions: a brief overview. Journal of Inclusion Phenomena and Macrocyclic Chemistry, 2012, 72, 1-14.	1.6	25
75	Controllable positions of Cu <sup>2+</sup> to enhance low-temperature SCR activity on novel Cu-Ce-La-SSZ-13 by a simple one-pot method. Chemical Communications, 2020, 56, 2360-2363.	4.1	25
76	Effect of adsorption properties of phosphorus-doped TiO2 nanotubes on photocatalytic NO removal. Journal of Colloid and Interface Science, 2019, 553, 647-654.	9.4	24
77	Effect of Core–Shell Support on Au/S-1/TS-1 for Direct Propylene Epoxidation and Design of Catalyst with Higher Activity. Industrial & Engineering Chemistry Research, 2019, 58, 4010-4016.	3.7	24
78	Mechanism study on TiO2 inducing O2- and O H radicals in O3/H2O2 system for high-efficiency NO oxidation. Journal of Hazardous Materials, 2020, 399, 123033.	12.4	24
79	The effects of calcination atmosphere on the catalytic performance of Ce-doped TiO <sub>2</sub> catalysts for selective catalytic reduction of NO with NH <sub>3</sub> . RSC Advances, 2017, 7, 23348-23354.	3.6	23
80	The solvent-driven formation of multi-morphological Ag–CeO <sub>2</sub> plasmonic photocatalysts with enhanced visible-light photocatalytic reduction of CO <sub>2</sub> . RSC Advances, 2018, 8, 40731-40739.	3.6	23
81	Anchoring CuS nanoparticles on accordion-like Ti <sub>3</sub> C <sub>2</sub> as high electrocatalytic activity counter electrodes for QDSSCs. Inorganic Chemistry Frontiers, 2020, 7, 3727-3734.	6.0	23
82	A CuO-V <sub>2</sub> O <sub>5</sub> /TiO <sub>2</sub> Catalyst for the Selective Catalytic Reduction of NO with NH <sub>3</sub> . Combustion Science and Technology, 2015, 187, 925-936.	2.3	22
83	Controllable synthesis of 3D BiVO <sub>4</sub> superstructures with visible-light-induced photocatalytic oxidation of NO in the gas phase and mechanistic analysis. Physical Chemistry Chemical Physics, 2015, 17, 28809-28817.	2.8	22
84	Modeling of ammonia-based wet flue gas desulfurization in the spray scrubber. Korean Journal of Chemical Engineering, 2011, 28, 1058-1064.	2.7	21
85	Facile synthesis of hierarchical nickel–cobalt sulfide quadrangular microtubes and its application in hybrid supercapacitors. Journal of Materials Science: Materials in Electronics, 2017, 28, 18064-18074.	2.2	21
86	Facile fabrication of oxygen and carbon co-doped carbon nitride nanosheets for efficient visible light photocatalytic H <sub>2</sub> evolution and CO <sub>2</sub> reduction. Dalton Transactions, 2019, 48, 12070-12079.	3.3	21
87	Facile Dynamic Synthesis of Homodispersed Ni <sub>3</sub> S <sub>2</sub> Nanosheets as a Highâ€Efficient Bifunctional Electrocatalyst for Water Splitting. ChemCatChem, 2019, 11, 1320-1327.	3.7	21
88	Promotional Effect of S Doping on V <sub>2</sub> O <sub>5</sub> –WO <sub>3</sub> /TiO <sub>2</sub> Catalysts for Low-Temperature NO <i><sub>x</sub></i> Reduction with NH <sub>3</sub> . Industrial & Engineering Chemistry Research, 2020, 59, 15478-15488.	3.7	20
89	TiO2 nanotube-supported V2O5 catalysts for selective NO reduction by NH3. Korean Journal of Chemical Engineering, 2013, 30, 836-841.	2.7	19
90	Cobalt supported on metal-doped ceria catalysts (M = Zr, Sn and Ti) for NO oxidation. RSC Advances, 2015, 5, 23193-23201.	3.6	19

#	Article	IF	CITATIONS
91	3D flower-like hierarchical Ag@nickel-cobalt hydroxide microsphere with enhanced electrochemical properties. Electronic Materials Letters, 2016, 12, 824-829.	2.2	19
92	H2S Solid oxide fuel cell based on a modified Barium cerate perovskite proton conductor. Ionics, 2009, 15, 385-388.	2.4	18
93	Preparation of nanosheet Fe-ZSM-5 catalysts, and effect of Fe content on acidity, water, and sulfur resistance in the selective catalytic reduction of NO x by ammonia. Research on Chemical Intermediates, 2013, 39, 4109-4120.	2.7	18
94	The effect of oxygen vacancies and fluorine dopant over adsorption behaviours of V2O5/TiO2 for NO removal. RSC Advances, 2014, 4, 5653.	3.6	18
95	Visible-Light-Driven Photoreduction of CO2 to CH4 with H2O Over Amine-Functionalized MIL-125(Ti). Catalysis Letters, 2019, 149, 3287-3295.	2.6	18
96	Partial substitution of magnesium in lanthanum manganite perovskite for nitric oxide oxidation: The effect of substitution sites. Journal of Colloid and Interface Science, 2020, 580, 49-55.	9.4	18
97	Highly efficient simulated solar-light photocatalytic oxidation of gaseous NO with porous carbon nitride from copolymerization with thymine and mechanistic analysis. RSC Advances, 2016, 6, 101208-101215.	3.6	17
98	The effects of nanoparticles on morphology and thermal properties of erythritol/polyvinyl alcohol phase change composite fibers. E-Polymers, 2018, 18, 321-329.	3.0	17
99	The utilization of dye wastewater in enhancing catalytic activity of CeO2-TiO2 mixed oxide catalyst for NO reduction and dichloromethane oxidation. Chemosphere, 2019, 235, 1146-1153.	8.2	17
100	Effect of oxygen vacancies and its quantity on photocatalytic oxidation performance of titanium dioxide for NO removal. Colloids and Surfaces A: Physicochemical and Engineering Aspects, 2021, 614, 126156.	4.7	17
101	Defect structure and evolution mechanism of O2â^' radical in F-doped V2O5/TiO2 catalysts. Colloids and Surfaces A: Physicochemical and Engineering Aspects, 2013, 436, 1013-1020.	4.7	16
102	Spinel Manganese–Cobalt Oxide on Carbon Nanotubes as Highly Efficient Catalysts for the Oxygen Reduction Reaction. Energy Technology, 2015, 3, 1183-1189.	3.8	16
103	Enhanced catalytic performance of F-doped CeO2–TiO2 catalysts in selective catalytic reduction of NO with NH3 at low temperatures. Research on Chemical Intermediates, 2015, 41, 3479-3490.	2.7	16
104	Spinel MnCo <sub>2</sub> O <sub>4</sub> /N,Sâ€doped Carbon Nanotubes as an Efficient Oxygen Reduction Reaction Electrocatalyst. ChemistrySelect, 2016, 1, 2159-2162.	1.5	16
105	Co(OH)2 particles decorated Ni3(NO3)1.6(CO3)0.2(OH)4 flower-like composite electrode for high-performance hybrid supercapacitors. Journal of Alloys and Compounds, 2020, 817, 152689.	5.5	16
106	Enhanced catalytic ozonation over reduced spinel CoMn <sub>2</sub> O <sub>4</sub> for NO <sub>x</sub> removal: active site and mechanism analysis. RSC Advances, 2016, 6, 115213-115221.	3.6	15
107	Synergistic Enhancement over Auâ€Pd/TSâ€1 Bimetallic Catalysts for Propylene Epoxidation with H 2 and O 2. ChemCatChem, 2019, 11, 5116-5123.	3.7	15
108	Ion-Exchanged ZIF-67 Synthesized by One-Step Method for Enhancement of CO <sub>2</sub> Adsorption. Journal of Nanomaterials, 2020, 2020, 1-11.	2.7	14

#	Article	IF	CITATIONS
109	A well-controlled three-dimensional tree-like core–shell structured electrode for flexible all-solid-state supercapacitors with favorable mechanical and electrochemical durability. Journal of Materials Chemistry A, 2021, 9, 16099-16107.	10.3	14
110	Modification of Catalytic Properties of Hollandite Manganese Oxide by Ag Intercalation for Oxidative Acetalization of Ethanol to Diethoxyethane. ACS Catalysis, 2021, 11, 5347-5357.	11.2	14
111	The chemical stability and conductivity improvement of protonic conductor BaCe0.8 â^ x Zr x Y0.2O3â Ionics, 2013, 19, 1745-1750.	€‰â^'â€% 2.4	bol´ <u>1</u> 3
112	Mesoporous TiO2 as the support of tetraethylenepentamine for CO2 capture from simulated flue gas. RSC Advances, 2013, 3, 23785.	3.6	13
113	Facile preparation of porous carbon nitride for visible light photocatalytic reduction and oxidation applications. Journal of Materials Science, 2018, 53, 11315-11328.	3.7	13
114	The Effect of CeO2 Dispersity and Active Oxygen Species on the SCR Reaction Over Fe-ZSM-5@Ce/meso-SiO2. Catalysis Letters, 2020, 150, 514-523.	2.6	13
115	Amorphousâ€crystalline Coâ^'Bâ^'P Catalyst for Synergistically Enhanced Hydrogen Evolution Reaction. ChemCatChem, 2020, 12, 6259-6264.	3.7	13
116	Promotional Effect of ZrO2 on supported FeCoK Catalysts for Ethylene Synthesis from catalytic CO2 hydrogenation. International Journal of Hydrogen Energy, 2020, 45, 15254-15262.	7.1	13
117	Insight into Deactivation Reasons for Nanogold Catalysts Used in Gas-Phase Epoxidation of Propylene. Catalysis Letters, 2020, 150, 1856-1864.	2.6	13
118	Flower-like 1T-MoS2/NiCo2S4 on a carbon cloth substrate as an efficient electrocatalyst for the hydrogen evolution reaction. Dalton Transactions, 2021, 50, 13320-13328.	3.3	12
119	Kinetics of Sulfite Oxidation in the Simultaneous Desulfurization and Denitrification of the Oxidationâ€Absorption Process. Chemical Engineering and Technology, 2015, 38, 797-803.	1.5	11
120	Hydrothermal Synthesis of Novel Uniform Nanooctahedral Bi <sub>3</sub> (FeO <sub>4</sub> )(WO <sub>4</sub> ) <sub>2</sub> Solid Oxide and Visible-Light Photocatalytic Performance. Industrial & Engineering Chemistry Research, 2016, 55, 12539-12546.	3.7	11
121	Composites of Single/Double Perovskites as Cathodes for Solid Oxide Fuel Cells. Energy Technology, 2016, 4, 804-808.	3.8	11
122	Metal–support interactions in Fe–Cu–K admixed with SAPO-34 catalysts for highly selective transformation of CO <sub>2</sub> and H <sub>2</sub> into lower olefins. Journal of Materials Chemistry A, 2021, 9, 21877-21887.	10.3	11
123	Foaming of polypropylene with supercritical carbon dioxide: An experimental and theoretical study on a new process. Journal of Applied Polymer Science, 2013, 130, 2877-2885.	2.6	10
124	A protophilic solventâ€assisted solvothermal approach to Cuâ€BTC for enhanced CO <sub>2</sub> capture. Applied Organometallic Chemistry, 2015, 29, 612-617.	3.5	10
125	Amorphous Core–Shell Nanoparticles as a Highly Effective and Stable Batteryâ€Type Electrode for Hybrid Supercapacitors. Advanced Materials Interfaces, 2019, 6, 1900858.	3.7	10
126	Dual-template assembled hierarchical Cu-SSZ-13: morphology evolution, crystal growth and stable high-temperature selective catalytic reduction performance. CrystEngComm, 2020, 22, 7036-7045.	2.6	10

#	Article	IF	CITATIONS
127	Formation of flaky carbon nitride and beta-Indium sulfide heterojunction with efficient separation of charge carriers for enhanced photocatalytic carbon dioxide reduction. Journal of Colloid and Interface Science, 2022, 611, 71-81.	9.4	10
128	Selective denitrification of flue gas by O3 and ethanol mixtures in a duct: Investigation of processes and mechanisms. Journal of Hazardous Materials, 2016, 311, 218-229.	12.4	9
129	Controllable synthesis of CeO <sub>2</sub> nanoparticles with different sizes and shapes and their application in NO oxidation. RSC Advances, 2016, 6, 50680-50687.	3.6	9
130	Mesoporous Spinel Nanofibers and Nitrogenâ€doped Carbon Nanotubes as Highâ€Performance Electrocatalyst for Oxygen Reduction in Alkaline and Neutral Media. Energy Technology, 2017, 5, 283-292.	3.8	9
131	A Rational Design for Enhanced Catalytic Activity and Durability: Strongly Coupled N-Doped CrOx/Ce0.2Zr0.8O2 Nanoparticle Composites. ACS Applied Nano Materials, 2018, 1, 1150-1163.	5.0	9
132	Effect of Small Nbâ€doping Amount on the Performance of BaCoO <sub>3â€Î´</sub> â€based Perovskite as Bifunctional Oxygen Catalysts. ChemistrySelect, 2018, 3, 12424-12429.	1.5	9
133	Effect of TS-1 Crystal Planes on the Catalytic Activity of Au/TS-1 for Direct Propylene Epoxidation with H <sub>2</sub> and O <sub>2</sub> . ACS Sustainable Chemistry and Engineering, 2020, 8, 8496-8504.	6.7	9
134	Tailorable boron-doped carbon nanotubes as high-efficiency counter electrodes for quantum dot sensitized solar cells. Catalysis Science and Technology, 2021, 11, 2745-2752.	4.1	9
135	The inhibition effect of oxygen inÂthe calcination atmosphere on the catalytic performance of MnOx–CeO2 catalysts for NO oxidation. Reaction Kinetics, Mechanisms and Catalysis, 2017, 122, 593-604.	1.7	8
136	Synthesis of 3D Hierarchical Rose-Like Bi2WO6 Superstructure with Enhanced Visible-Light-Induced Photocatalytic Performance. Jom, 2019, 71, 2112-2119.	1.9	8
137	Dynamic Restructuring of Cuâ€Doped SnS <sub>2</sub> Nanoflowers for Highly Selective Electrochemical CO <sub>2</sub> Reduction to Formate. Angewandte Chemie, 2021, 133, 26437-26441.	2.0	8
138	Insight into the surface property modification-enhanced C <sub>3</sub> N <sub>4</sub> performance of photocatalytic nitrogen fixation. Chemical Communications, 2022, 58, 6502-6505.	4.1	8
139	Structures and Catalytic Properties of Lithium Phosphates. Catalysis Letters, 2011, 141, 1032-1036.	2.6	7
140	Coral-Like CoSe <sub>2</sub> -Nitrogen-Doped Porous Carbon as Efficient Counter Electrodes for Quantum Dot Sensitized Solar Cells. ECS Journal of Solid State Science and Technology, 2021, 10, 045012.	1.8	7
141	Using the OSPM model on pollutant dispersion in an urban street canyon. Advances in Atmospheric Sciences, 2010, 27, 621-628.	4.3	6
142	Simulation of Hydrogen Production in Biomass Gasifier by ASPEN PLUS. , 2010, , .		6
143	Effect of an anode modified with nitrogenous compounds on the performance of a microbial fuel cell. Energy Sources, Part A: Recovery, Utilization and Environmental Effects, 2016, 38, 527-533.	2.3	6
144	Efficient Inhibition of N <sub>2</sub> O during NO Absorption Process Using a CuO and (NH <sub>4</sub> ) <sub>2</sub> SO <sub>3</sub> Mixed Solution. Industrial & Engineering Chemistry Research, 2018, 57, 13010-13018.	3.7	6

#	Article	IF	CITATIONS
145	In situ fabrication of cobalt/nickel sulfides nanohybrid based on various sulfur sources as highly efficient bifunctional electrocatalysts for overall water splitting. Nano Select, 0, , .	3.7	6
146	Plasmonic Ag Nanoparticles Decorated Acid-Aching Carbon Fibers for Enhanced Photocatalytic Reduction of CO2 into CH3OH Under Visible-Light Irradiation. Catalysis Letters, 2021, 151, 3079-3088.	2.6	6
147	Synergistic Pd/Cu-catalysed regio- and stereoselective borylation of allenylic carbonates. Chemical Communications, 2022, 58, 1037-1040.	4.1	6
148	Catalytic Performances of Hollow Li <sub>3</sub> PO <sub>4</sub> Spheres for Propylene Oxide Isomerization. Chemical Engineering Communications, 2016, 203, 339-344.	2.6	5
149	Understanding the Effect of Germanium as an Efficient Auxiliary Preâ€Dopant in Carbon Nanotubes on Enhancing Oxygen Reduction Reaction. Energy Technology, 2018, 6, 2387-2393.	3.8	5
150	Fabrication of core–shell C/MnO nanocomposite by liquid deposition for high performance lithium-ion batteries. Journal of Materials Science: Materials in Electronics, 2019, 30, 5978-5985.	2.2	5
151	Microreactor technology for synthesis of ethyl methyl oxalate from diethyl oxalate with methanol and its kinectics. Canadian Journal of Chemical Engineering, 2020, 98, 2321-2329.	1.7	5
152	Glucose-derived porous carbon as a highly efficient and low-cost counter electrode for quantum dot-sensitized solar cells. New Journal of Chemistry, 2020, 44, 6362-6368.	2.8	5
153	Highly-dispersed CoS2/N-doped carbon nanoparticles anchored on RGO skeleton as a hierarchical composite counter electrode for quantum dot sensitized solar cells. Chemical Engineering Journal, 2022, 430, 132732.	12.7	5
154	Synthesis and performance of Sm0.9Sr0.1Cr0.5Fe0.5O3 as anode material for SOFCs running on H2S-containing fuel. Ionics, 2013, 19, 491-497.	2.4	4
155	Foaming of Homogeneous Polypropylene and Ethylene-Polypropylene Block Copolymer Using Supercritical Carbon Dioxide. Polymer-Plastics Technology and Engineering, 2013, 52, 592-598.	1.9	4
156	Orthogonal Design Study on Factors Affecting Foaming Behaviors of Polypropylene and Polypropylene/Nano-Calcium Carbonate Nanocomposites. Polymer-Plastics Technology and Engineering, 2013, 52, 7-15.	1.9	4
157	Synthesis and characterization of Ca and Sr co-doped ceria electrolytes. Ionics, 2014, 20, 721-727.	2.4	4
158	Improvement of BaCe0.8Sm0.1Y0.1O3-δ-based IT-SOFC by optimizing spin-coated process of cathode and sintering temperature. Ionics, 2015, 21, 817-822.	2.4	4
159	Steam treatment of a hollow lithium phosphate catalyst: enhancing carbon deposition resistance and improving the catalytic performance of propylene oxide rearrangement. RSC Advances, 2016, 6, 57000-57008.	3.6	4
160	The Role of Lewis and BrÃ,nsted Acid Sites in NO Reduction with NH3 on Sulfur Modified TiO2-Supported V2O5 Catalyst. Russian Journal of Physical Chemistry A, 2017, 91, 2489-2494.	0.6	4
161	CrOx Anchored on the Black-TiO2 Surface via Organic Carboxylic Acid Ligand and Its Catalysis in Oxidation of NO. Catalysis Letters, 2021, 151, 1755-1765.	2.6	4
162	Fe-Co-K/ZrO <sub>2</sub> Catalytic Performance of CO <sub>2</sub> Hydrogenation to Light Olefins. Wuji Cailiao Xuebao/Journal of Inorganic Materials, 2021, 36, 1053.	1.3	4

#	Article	IF	CITATIONS
163	Enhanced Light-driven CO2 Reduction on Metal-free Rich Terminal Oxygen-defects Carbon Nitride Nanosheets. Journal of Colloid and Interface Science, 2021, 608, 2505-2505.	9.4	4
164	Mechanism and Kinetic Study of Cyclodextrin Use to Facilitate NO <sub>2</sub> Absorption in Sulfite Solutions. Environmental Science & Solutions, 2022, 56, 7696-7706.	10.0	4
165	Investigation of Ce0.9Sr0.1Cr0.5Co0.5O3â^î^â as the anode material for solid oxide fuel cells fueled with H2S. Ionics, 2014, 20, 1011-1021.	2.4	3
166	Synergetic effects of surface free Co <sub>3</sub> O <sub>4</sub> species on catalytic oxidation of NO over cerium-cobalt solid solution. Journal of Dispersion Science and Technology, 2020, 41, 1976-1983.	2.4	3
167	Engineering application of desulfurization and denitrification comprehensive purification technology for activated coke. Environmental Progress and Sustainable Energy, 2021, 40, e13642.	2.3	3
168	Carbonâ€Based Electrocatalysts for Efficient Hydrogen Peroxide Production (Adv. Mater. 49/2021). Advanced Materials, 2021, 33, .	21.0	3
169	Ce0.9Sr0.1Cr0.5Mn0.5O3â^^î^ as the anode materials for solid oxide fuel cells running on H2 and H2S. Korean Journal of Chemical Engineering, 2011, 28, 1764-1769.	2.7	2
170	Performance and sulfur resistance of doped yttrium chromite-ceria composite as anode material for the SOFCs operating on H2S-containing fuel. Ionics, 2016, 22, 1415-1424.	2.4	2
171	Effect of pre-oxidation process on V2O5/AC catalyst for the selective catalytic reduction of NOx with NH3. Environmental Science and Pollution Research, 2022, 29, 13534-13540.	5.3	2
172	Improving the electrocatalytic activity and stability of spinel sulfide counter electrodes by trimetallic synergy effects for quantum dot sensitized solar cells. New Journal of Chemistry, 2021, 45, 4766-4772.	2.8	2
173	Fabrication of Controllable N-Doped Ce0.2Zr0.8O2 via O–N–O Bond with Robust NO Oxidation and Durability at Low Temperature. Energy & Fuels, 2021, 35, 752-761.	5.1	2
174	FeZnK/SAPO-34 Catalyst for Efficient Conversion of CO2 to Light Olefins. Catalysis Letters, 2023, 153, 54-61.	2.6	2
175	The Catalytic Activity of F-Doped Vanadia/Titania Catalysts for Selective Catalytic Reduction of NO with NH3 at Low Temperatures. , 2009, , .		1
176	Electrocatalysis: Porous Cobalt Phosphide Polyhedrons with Iron Doping as an Efficient Bifunctional Electrocatalyst (Small 40/2017). Small, 2017, 13, .	10.0	1
177	Nitrogen Oxide Decomposition on Cerium Modified ZSM-5 Zeolite in the Presence of Oxygen. , 2009, , .		0
178	The Impact of Building Configuration and Wall Heating on Pollutant Dispersion in Urban Street Canyon. International Conference on Bioinformatics and Biomedical Engineering: [proceedings] International Conference on Bioinformatics and Biomedical Engineering, 2010, , .	0.0	0
179	Ce0.8Sr0.2Cr0.5V0.5 as the anode materials for H2S fueled solid oxide fuel cells. , 2010, , .		0
180	Electro-chemical Properties Comparison and Application in Water-treatment of Different DSA Anodes. , 2012, , .		0

#	Article	IF	CITATIONS
181	Purification of Polyether Polyols with Low Unsaturation. Advanced Materials Research, 0, 781-784, 2361-2365.	0.3	ο
182	NCoCu Carbon Dots Intertwined NiCo Double Hydroxide Nanorod Array for Efficient Electrocatalytic Hydrogen Evolution. ChemCatChem, 2021, 13, 4714-4723.	3.7	0